THE JOURNAL OF BIOLOGICAL CHEMISTRY VOL. 288, NO. 33, pp. 23884–23892, August 16, 2013
© 2013 by The American Society for Biochemistry and Molecular Biology, Inc. Published in the U.S.A.

Copper Import into the Mitochondrial Matrix in *Saccharomyces cerevisiae* Is Mediated by Pic2, a Mitochondrial Carrier Family Protein*

Received for publication, March 19, 2013, and in revised form, July 2, 2013 Published, JBC Papers in Press, July 11, 2013, DOI 10.1074/jbc.M113.470674

Katherine E. Vest[‡], **Scot C. Leary**[§], **Dennis R. Winge**[¶], **and Paul A. Cobine**[‡1]

From the [‡]*Department of Biological Sciences, Auburn University, Auburn, Alabama 36849, the* [§]*Department of Biochemistry, University of Saskatchewan, Saskatoon, Saskatchewan S7N 5E5, Canada, and the* [¶]*Departments of Biochemistry and Medicine, University of Utah, Salt Lake City, Utah 84132*

Background: Copper must enter the mitochondrial matrix prior to assembly into cytochrome *c* oxidase.
Results: Pic2 transports mitochondrial copper *in vivo* and *in vitro*.
Conclusion: Pic2 mediates copper import into the mitochondrial matrix.
Significance: We have identified the first mitochondrial copper importer.

Saccharomyces cerevisiae **must import copper into the mitochondrial matrix for eventual assembly of cytochrome *c* oxidase. This copper is bound to an anionic fluorescent molecule known as the copper ligand (CuL). Here, we identify for the first time a mitochondrial carrier family protein capable of importing copper into the matrix. *In vitro* transport of the CuL into the mitochondrial matrix was saturable and temperature-dependent. Strains with a deletion of *PIC2* grew poorly on copper-deficient non-fermentable medium supplemented with silver and under respiratory conditions when challenged with a matrix-targeted copper competitor. Mitochondria from *pic2*Δ cells had lower total mitochondrial copper and exhibited a decreased capacity for copper uptake. Heterologous expression of Pic2 in *Lactococcus lactis* significantly enhanced CuL transport into these cells. Therefore, we propose a novel role for Pic2 in copper import into mitochondria.**

Metals are essential nutrients that pose a management quandary for cells. They must be directed to the correct proteins and organelles through a maze of cellular components and opportunistic metal-binding sites (1). Failure to control their delivery results in cellular stress, presumably due to inappropriate interactions and oxidative damage. Cells have adopted a protein-mediated delivery mechanism for copper within the cytosol. In the budding yeast *Saccharomyces cerevisiae*, copper enters the cell via specific (Ctr1) and nonspecific (*e.g.* Fet4) transporters and is then trafficked to points of utilization by copper chaperone proteins (2). Copper is used as a cofactor in three major enzymes: the multicopper oxidase Fet3 required for high affinity iron uptake (3); Sod1, a Cu,Zn-superoxide dismutase required for protection against oxidative stress and regulation of glucose signaling in yeast (4); and cytochrome *c* oxidase (CcO),[2] the terminal enzyme complex of the electron transport chain (5). Atx1 is the copper chaperone responsible for delivering copper to the *trans*-Golgi vesicles via Ccc2, a P-type ATPase (6), whereas Ccs1 serves as the copper donor for Sod1 and acts as a post-transfer modifying enzyme by facilitating the formation of an essential disulfide bond within the enzyme itself (7). Although cytosolic copper trafficking has been well characterized, the pathway that delivers copper to mitochondria in yeast and in other eukaryotes is completely unknown.

CcO is a multimeric protein complex that contains two copper centers, a binuclear Cu_A site and a heme a_3-Cu_B site. A number of assembly factors act in concert to build both of these sites. The soluble intermembrane space (IMS) protein Cox17 delivers copper to both Sco1 and Cox11, which are integral inner membrane (IM) proteins that donate copper to the assembling holoenzyme (8, 9). Additionally, the IMS protein Cmc1 has been implicated in the control of copper flow within the IMS, potentially by directing copper to the Cox17-mediated CcO assembly pathway (10).

Organellar fractionation experiments showed that >70% of mitochondrial copper is present as a soluble anionic complex contained within a matrix-localized bioavailable pool (11). This complex has been defined as the copper ligand (CuL), and its existence and localization have since been confirmed by x-ray fluorescence imaging and copper chelation studies (12, 13). Copper-dependent human SOD1 localized to this mitochondrial compartment is able to rescue a range of phenotypic defects associated with *SOD2* deletion, demonstrating the accessibility of this pool (11). Expression of matrix-targeted human SOD1 or yeast Crs5, a copper-binding metallothionein, results in a specific loss of CcO activity that can be rescued by addition of copper or decreased expression of the competing cuproprotein (14). These observations led us to propose that

* This work was supported, in whole or in part, by National Institutes of Health GM083292 (to D. R. W.). This work was also supported by National Science Foundation Grant BIO-MCB-1158497 (to P. A. C.) and by Saskatchewan Health Research Foundation Establishment and Natural Sciences and Engineering Research Discovery grants (to S. C. L.).

[1] To whom correspondence should be addressed: Dept. of Biological Sciences, 101 Rouse Life Sciences, Auburn University, Auburn, AL 36849. Tel.: 344-844-1661; E-mail: paul.cobine@auburn.edu.

[2] The abbreviations used are: CcO cytochrome *c* oxidase; IMS, intermembrane space; IM, inner membrane; CuL, copper ligand; MCF, mitochondrial carrier family; BCS, bathocuproinedisulfonic acid; AgL, silver ligand; ICP-OES, inductively coupled plasma optical emission spectroscopy; hSOD1, human SOD1.

the matrix copper pool is redistributed to the IMS, where it is made available to CcO. Although the exact structural identity of the CuL is unknown, we have characterized many aspects of its *in vivo* function. We propose that the ligand exists in a metal-free form in the cytosol, where it binds copper and delivers it to mitochondria, providing a non-proteinaceous trafficking system for copper delivery to the organelle.

The IM is impermeable to most ions and molecules, so transporters must exist that facilitate matrix import of the CuL complex and its subsequent redistribution to the IMS. However, transporters required for the movement of copper across the IM have yet to be identified and remain a fundamental gap in our understanding of the mechanisms that provide for the assembly of CcO. Data from our previous studies suggest that the CuL is the molecule that is transported into the matrix and that this complex may resemble a metabolite or nucleotide. Therefore, copper transport across the IM may proceed through one or more of the mitochondrial carrier family (MCF) proteins. These proteins transport diverse metabolic substrates, such as oxaloacetate, citrate, GTP, and ATP, into and out of the matrix (15).

MCF proteins have been previously implicated in metal ion homeostasis (16). High affinity iron uptake into mitochondria of *S. cerevisiae* is disrupted by simultaneous deletion of *MRS3* and *MRS4* (17). Studies of the Mrs3/4 homologs in vertebrate systems have demonstrated the conserved function of these proteins (18–22). Other members of this family have also been associated with iron transport with varying levels of specificity (23–26). Therefore, a precedent exists for the involvement of multiple MCF proteins in modulating mitochondrial metal ion homeostasis. Herein, we present evidence that the MCF protein Pic2 transports copper across the mitochondrial IM, allowing for its accumulation within the matrix.

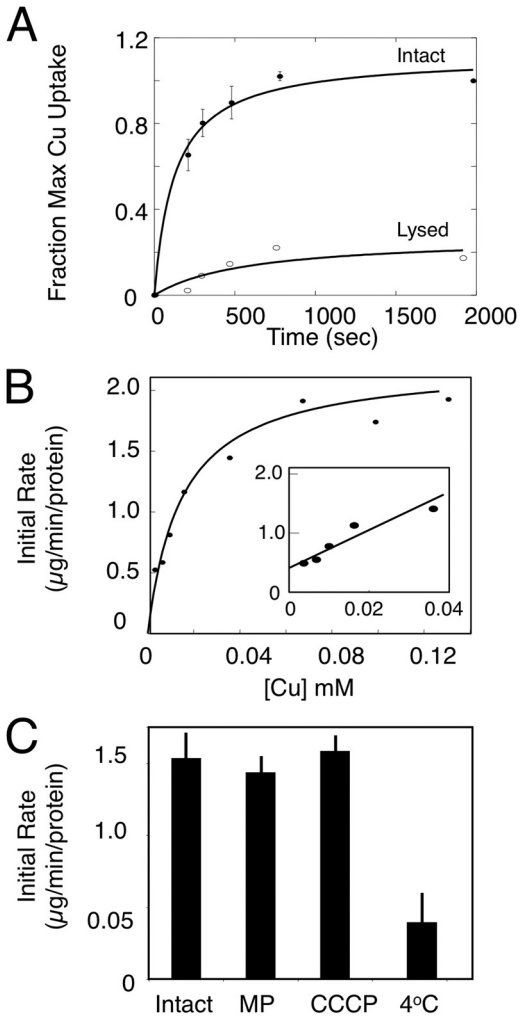

FIGURE 1. ***In vitro* CuL uptake in purified mitochondria.** *A*, intact mitochondria were incubated with purified CuL and isolated by centrifugation, and copper was measured by ICP-OES. Fraction of maximal uptake is plotted *versus* incubation time for an average of three independent experiments with wild-type mitochondria. *Error bars* represent S.D. *B*, initial rates of uptake across a range of CuL concentrations. Data are fit by a hyperbolic curve. The *inset* shows the initial rate of uptake at 0–50 μM CuL and is fitted by linear regression. *C*, the initial rate of CuL uptake was measured by ICP-OES in intact mitochondria, mitoplasts (*MP*) were prepared by hypotonic lysis, and mitochondria were incubated with the uncoupler carbonyl cyanide *m*-chlorophenylhydrazone (*CCCP*) or were incubated at 4 °C. The means ± S.D. are shown for three independent experiments.

EXPERIMENTAL PROCEDURES

Yeast Strains, Culture Conditions, and Standard Methods—The yeast strains used in this study were BY4741 (*MAT***a** *leu2*Δ *met15*Δ *ura3*Δ *his3*Δ) and the isogenic kanMX4-containing mutant from Invitrogen. *ccs1*Δ::*IMhSOD1* was created in the Y7092 background (*MAT*α *can1*Δ::*STE2pr-Sp_his5 lyp1*Δ *his3*Δ *leu2*Δ *ura3*Δ *met15*Δ) (27). All cultures were grown in YP medium (1% yeast extract and 2% peptone) or synthetic defined media (with selective amino acids excluded) with the appropriate filter-sterilized carbon source added. Metal concentrations were varied using BIO 101 yeast nitrogen base (Sunrise Science Products) plus added 0.1 mM ferrous chloride to give copper-deficient conditions. If required, further copper chelation was achieved by adding bathocuproinedisulfonic acid (BCS). Exogenous copper was provided by adding $CuSO_4$. All of the growth tests were performed at 30 °C with 1:10 serial dilutions of precultures grown under permissive conditions.

Vector Constructs—Matrix-targeted Crs5 was described previously (14). The *PIC2*/*YER053C* ORF plus 300 bp upstream (to include the endogenous promoter) was cloned into pRS415. The *PIC2* ORF was also cloned into pNZ8148 (MoBiTec) under the control of the nisin-inducible promoter. The fidelity of each construct was verified by dideoxynucleotide sequencing prior to use.

Isolation of the CuL and Silver Ligand (AgL) from Mitochondria—Intact mitochondria were prepared, and the resultant soluble contents were fractionated as described previously (11). Anionic fractions for reverse phase chromatography were prepared by adding DEAE resin (Whatman) in batch. The resin was washed with 25 bed volumes of 20 mM ammonium acetate (pH 8.0) and eluted with 5 volumes of 1 M ammonium acetate (pH 8.0). The samples were loaded directly onto a Phenomenex C_{18} column. Unbound fractions were removed with 50 mM ammonium acetate (pH 5.0) or with 0.1% trifluoroacetic acid to isolate the apo-ligand. A 60-min gradient to 100% acetonitrile was used, and 1-ml fractions were collected. The final fractions were analyzed for copper by inductively coupled plasma optical emission spectroscopy (ICP-OES; PerkinElmer Life Sciences 9300-DV system) and for fluorescence (PerkinElmer Life Sci-

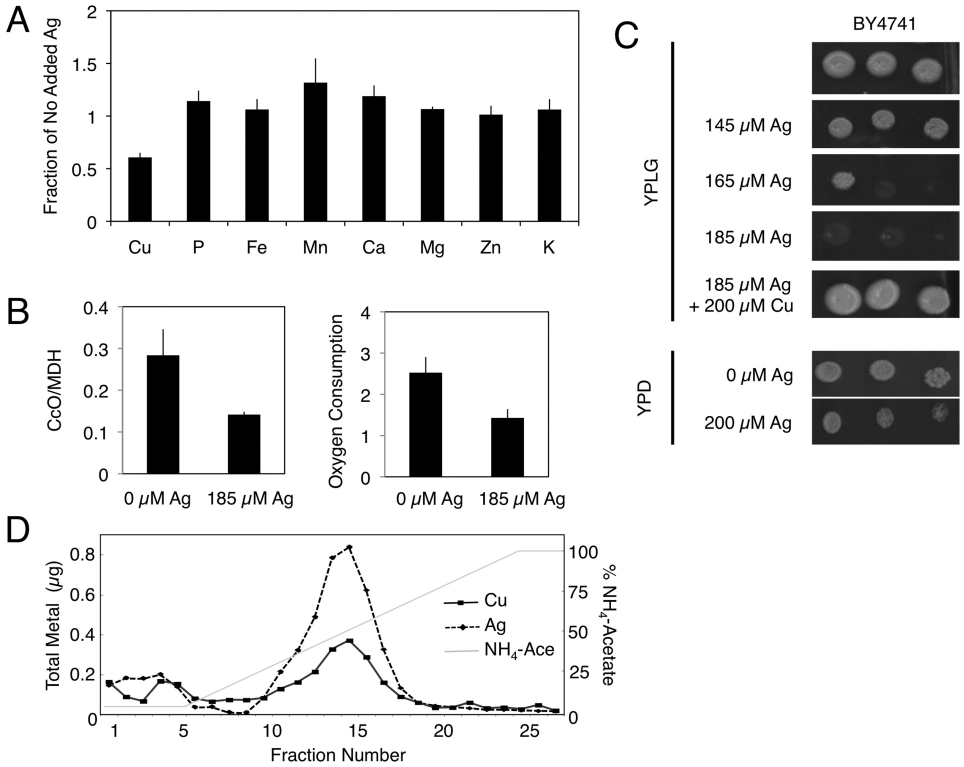

FIGURE 2. **Silver accumulates in yeast mitochondria.** *A*, the mineral element content of purified mitochondria from BY4741 yeast cultured in the absence or presence of 185 μM silver was quantified by ICP-OES and is expressed as a ratio (*i.e.* with silver/without silver). The means ± S.D. of three independent cultures and mitochondrial preparations are shown. *B*, CcO activity of purified mitochondria from *A* and oxygen consumption of whole cells cultured in YP/galactose medium without or with 185 μM silver. *C*, serial dilutions of BY4741 yeast grown in rich medium with a fermentable carbon source (YPD medium (YP medium containing glucose)) or with a non-fermentable carbon source (YPLG medium (YP medium containing lactate and glycerol)) in the presence of the cell-impermeable copper chelator BCS and increasing silver concentrations. The growth defect was reversed by addition of copper to the BCS- and silver-supplemented plates. *D*, anion exchange fractionation of soluble contents from purified mitochondria isolated from cultures grown in 185 μM silver. Copper (■) and silver (♦) were measured by ICP-OES. *NH_4-Ace*, ammonium acetate.

ences LS55 fluorometer). Excitation and emission scans of copper-containing fractions were performed at an excitation maximum of 220 nm and an emission maximum of 360 nm using 5-nm slit widths.

Pic2 Expression in Lactococcus lactis—*L. lactis* cells transformed with vector (pNZ8148) alone or carrying the *PIC2* gene were grown overnight at 30 °C in M17 medium with 0.5% glucose and 10 μg/ml chloramphenicol. Cells were diluted into fresh medium at an A_{600} of 0.1, grown to an A_{600} of 0.4, and induced using 1 ng/ml nisin for 5 h. Protein expression was confirmed using SDS-PAGE, followed by SYPRO staining or immunoblotting for Pic2.

Copper Uptake Assays—Isolated mitochondria suspended in 0.6 M sorbitol were incubated with the CuL for 30-s intervals and removed from the solution by centrifugation. Uptake was measured by ICP-OES as an increase in copper over time. Copper uptake was assayed in *L. lactis* using a modified method in which whole cells were resuspended in soluble matrix copper, purified ligand, or copper salts in either water or potassium phosphate buffer (pH 7.5). Cells were incubated for different time points at room temperature, removed by centrifugation, and washed with water, and total metals were measured by ICP-OES. Uptake is reported as the increase in copper over time.

Enzyme Assay—CcO and malate dehydrogenase activities were measured as described previously (11) using a Shimadzu UV-2450 system. Superoxide dismutase (SOD1) activity was measured using a xanthine oxidase-linked assay kit (Sigma).

Miscellaneous Methods—The anti-human SOD1 monoclonal antibody was purchased from Santa Cruz Biotechnology. Antisera for Cox2 (cytochrome *c* oxidase subunit 2) and porin were purchased from Invitrogen. Antiserum for yeast Pic2 was raised against a synthetic peptide consisting of the 20 N-terminal residues (GenScript).

RESULTS

Copper Transport into Isolated Mitochondria—We assume that the transported form of copper into mitochondria is the CuL complex. To assess transport characteristics into yeast mitochondria, we isolated the soluble matrix copper contents using anion exchange resin and incubated purified intact mitochondria with variable concentrations of the stable CuL complex. Mitochondria were removed by centrifugation and then assayed for their total copper content by ICP-OES. The CuL was imported into mitochondria in a time-dependent manner (Fig. 1*A*). The observed increase in copper content was not due to membrane association, as lysis of mitochondria via sonication before assay prevented accumulation (Fig. 1*A*), and lysis after uptake released the copper into the soluble fraction (80 ± 5% soluble). Increasing concentrations of the CuL complex saturated the initial rate of copper uptake (Fig. 1*B*). Half-maximal transport was observed at ~15 μM CuL complex. Uptake was

temperature-dependent, as incubation of mitochondria at 4 °C prevented CuL accumulation, and identical initial rates were obtained in mitoplasts lacking the outer membrane (Fig. 1*C*), suggesting that the transport occurred at the IM. Addition of the uncoupling ionophore carbonyl cyanide *m*-chlorophenylhydrazone did not affect the initial rates of uptake (Fig. 1*C*). Therefore, we conclude that the mitochondrial IM has a saturable temperature-dependent copper transport system.

The AgL Complex Acts as a Competitor for Copper Uptake—External chelators are often used to deplete the medium of copper. However, we sought to find a competitor that could more directly affect mitochondrial copper. Silver shares similar electronic properties with copper, and it is often used as a toxic mimetic of copper in biological systems (28, 29). We therefore isolated intact mitochondria from yeast grown in glucose-containing medium with or without 185 μM $AgNO_3$. Mitochondria from cells grown in the presence of silver accumulated 17 ± 0.4 mmol of silver/mol of sulfur and contained 3.3 ± 0.2 mmol of copper/mol of sulfur, whereas mitochondria from untreated cells contained 5.4 ± 0.1 mmol of copper/mol of sulfur. Although the mitochondrial copper content was reduced in silver-treated cultures, the other mineral element concentrations were comparable to those in the untreated cultures (Fig. 2*A*). The decrease in copper was associated with a decrease in CcO activity and oxygen consumption (Fig. 2*B*). Separate cultures were grown in medium containing either 150 μM silver or 150 μM copper. Under these identical conditions, silver accumulated to ~5-fold higher concentrations in mitochondria compared with copper (data not shown). Moreover, addition of 185 μM silver to rich medium containing a non-fermentable carbon source limited the growth of wild-type cells (Fig. 2*C*). Mitochondria from these silver-treated cells were fractionated into soluble and insoluble components, and the soluble contents were separated by anion exchange chromatography (Fig. 2*D*). The fractions containing the CuL also contained an anionic silver complex (AgL).

Anionic AgL was used for *in vitro* uptake assays. Like the CuL, the AgL complex was imported into mitochondria in a time- and concentration-dependent manner (Fig. 3*A*). On the basis of the *in vivo* observation that silver affected copper accumulation in mitochondria, we attempted to mimic this *in vitro*. The AgL complex was added to mitochondria in 10-fold excess compared with the CuL, and the initial rate of uptake was monitored. The excess AgL acted as a competitor, greatly decreasing CuL uptake (Fig. 3*B*). Conversely, a 10-fold excess of the CuL slowed uptake of the AgL into mitochondria (Fig. 3*C*).

Deletion of PIC2 Results in Copper-related Phenotypes—Yeast lacking *PIC2*, which encodes a MCF protein, had a growth defect on non-fermentable medium in the presence of the cell-impermeable copper chelator BCS. This defect was exacerbated by addition of silver to the medium and reversed upon addition of copper (Fig. 4*A*). The decrease in growth was accompanied by a silver-dependent depletion of Cox2 protein in these mitochondria (Fig. 4*B*). The *pic2*Δ strain also showed a defect on copper-limited synthetic medium with a non-fermentable carbon source without addition of silver (Fig. 5*A*). In agreement with the growth phenotype, we observed a 50% reduction in CcO activity and oxygen consumption in the *pic2*Δ mutant (Fig. 5*B*). To exaggerate the growth defect in the *pic2*Δ strain, we transformed the cells with a matrix-targeted copper metallothionein (*CRS5*) that we have used previously to biochemically deplete the bioavailable matrix copper pool (14). The *pic2*Δ strain expressing matrix-targeted *CRS5* exhibited a greater growth defect compared with the *pic2*Δ strain alone on copper-replete non-fermentable medium, a defect that became more severe upon depletion of available copper from the medium by addition of increasing BCS concentrations (Fig. 5*C*).

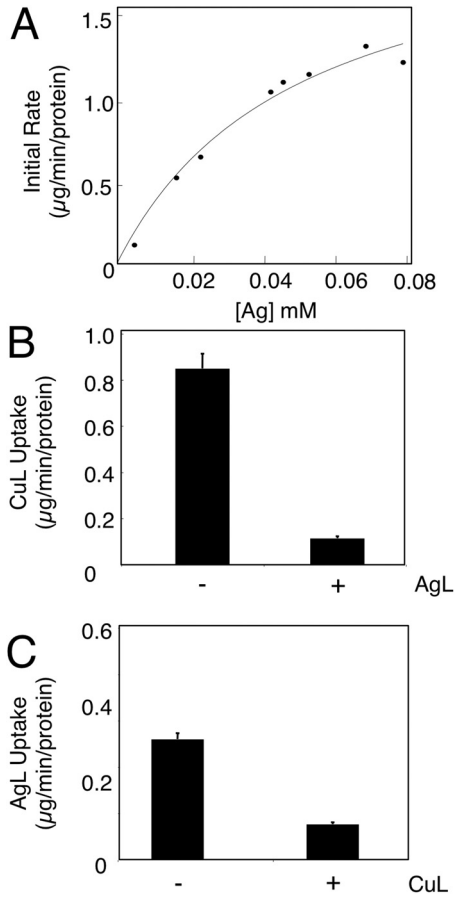

FIGURE 3. ***In vitro* AgL uptake into purified mitochondria.** *A*, intact mitochondria were incubated with purified AgL and isolated by centrifugation, and silver was measured by ICP-OES. The initial rates of uptake are plotted against a range of AgL concentrations. A hyperbolic curve is fitted. *B*, the initial rate of CuL uptake at 10 μM CuL was measured by ICP-OES in intact mitochondria in the presence of 100 μM AgL ($n = 5$). *C*, the initial rate of AgL uptake with 10 μM AgL was measured by ICP-OES in intact mitochondria in the presence of 100 μM CuL ($n = 5$).

To monitor mitochondrial copper homeostasis without confounding factors related to translation or the activity of other chaperone proteins, we used the previously described copper/IMS biomarker strain (14). In this biomarker strain, the gene for the copper chaperone for Sod1, *CCS1*, has been deleted, rendering the yeast *Sod1* inactive and causing a lysine auxotrophy. An IM-tethered human *SOD1* (*IM-hSOD1*) is then stably expressed and rescues the Sod1 deficit of the *ccs1*Δ strain in a manner that is dependent on matrix copper being made available within the IMS. Although deletion of *PIC2* did not change the steady-state levels of IM-hSOD1 (Fig. 6*A*), SOD1 activity in BCS-supplemented medium was decreased to 39% of the parental strain (Fig. 6*B*). Supplementation of the medium with

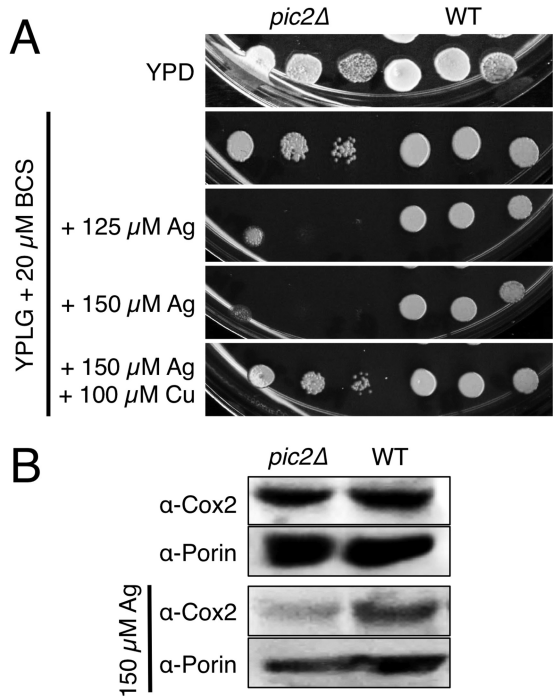

FIGURE 4. **Silver-related growth phenotypes of *pic2*Δ yeast strains.** *A*, serial dilutions of BY4741 and *pic2*Δ strains grown in rich medium with a fermentable carbon source (YPD medium) or with a non-fermentable carbon source (YPLG medium) in the presence of the cell-impermeable copper chelator BCS and increasing silver concentrations. The growth defect was reversed by addition of copper to the BCS- and silver-supplemented plates. *B*, Western blots for Cox2 in mitochondria isolated from cells grown in rich medium with a fermentable carbon source (*upper panel*) or in identical medium supplemented with 150 μM silver (*lower panel*). Porin served as an internal loading control.

silver progressively decreased the activity of IM-hSOD1 in *ccs1*Δ mitochondria, and deletion of *PIC2* exacerbated this defect (Fig. 6*C*). These data strongly suggest that mitochondrial copper required for the metallation of IMS cuproenzymes is a limiting factor in *pic2*Δ cells.

*Biochemical Characterization of pic2*Δ *Mitochondria*—Mitochondria isolated from *pic2*Δ cells grown in synthetic medium were analyzed for total metals by ICP-OES and showed a mild decrease in copper to 0.7-fold of the parental strain (1.9 ± 0.2 mmol of copper/mol of sulfur in the parental strain *versus* 1.2 ± 0.2 mmol of copper/mol of sulfur in *pic2*Δ mitochondria). To exaggerate this phenotypic effect, *pic2*Δ cells were grown in synthetic medium with added 0.5 mM $CuSO_4$, and the mineral profile of the mitochondria was compared with that of parental yeast cultured under the same conditions (Fig. 7*A*). Although both strains had increased mitochondrial copper under these conditions, the *pic2*Δ mitochondria accumulated less copper compared with the parental strain (~0.4-fold). There was no observable change in the content of phosphorus, iron, manganese, calcium, and magnesium, but we observed an ~1.5-fold increase in zinc and potassium. These data suggest a specific defect in copper uptake in *pic2*Δ mitochondria (Fig. 7*A*).

Intact mitochondria from *pic2*Δ cells were incubated with purified CuL complex and assayed for uptake. Initial rates of CuL uptake were decreased in *pic2*Δ mitochondria relative to those in parental cells (Fig. 7*B*). Moreover, *pic2*Δ mitochondria showed lower maximal rates of uptake. This change in satura-

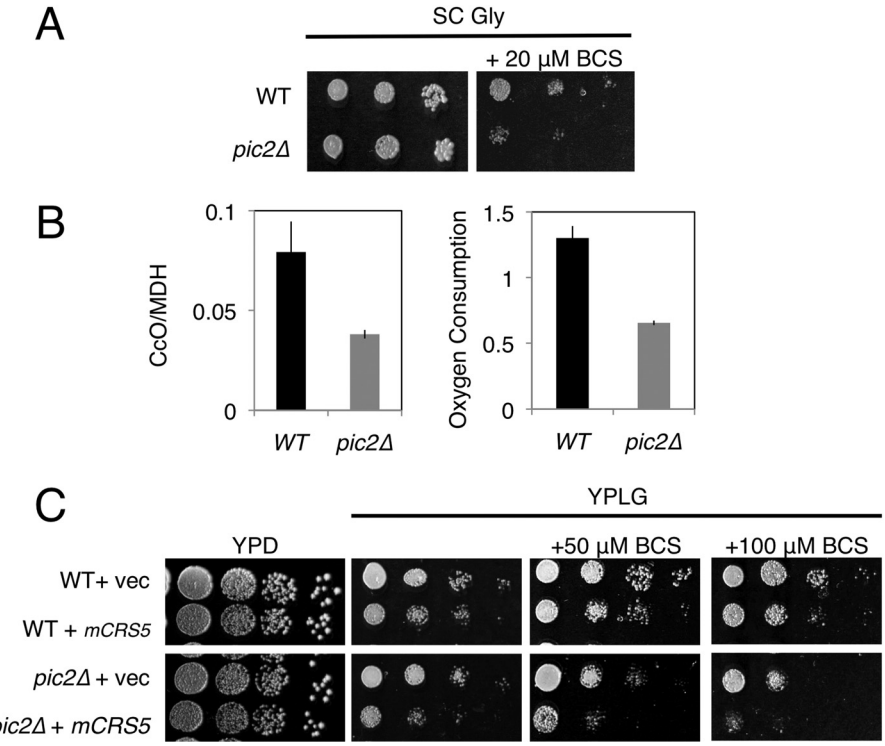

FIGURE 5. **Growth phenotypes of *pic2*Δ yeast strains upon copper depletion.** *A*, serial dilutions of BY4741 and *pic2*Δ strains grown in synthetic medium with a non-fermentable carbon source (glycerol; *SC Gly*) with or without 20 μM BCS. *B*, *left panel*, CcO activity in mitochondria isolated from parental and *pic2*Δ strains grown in synthetic medium containing galactose as a carbon source. *MDH*, malate dehydrogenase. *Right panel*, oxygen consumption read as percent air/A_{600}/s of whole cells from each strain grown in galactose-containing rich medium ($n = 3$). *C*, serial dilutions of parental and *pic2*Δ strains transformed with either empty vector (*vec*) or matrix-targeted *CRS5* (*mCRS5*) on rich medium with a fermentable carbon source (YPD medium), with a non-fermentable carbon source (YPLG medium), or YPLG medium with limited copper availability (+50 μM BCS and +100 μM BCS).

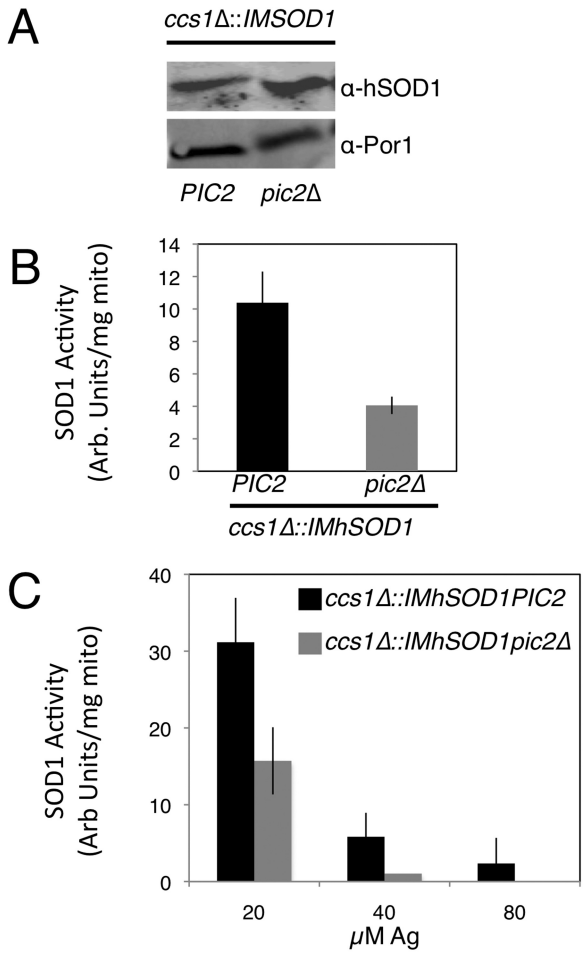

FIGURE 6. **Deletion of *PIC2* limits hSOD1 activity in a *ccs1*Δ::*IMhSOD1* reporter strain.** *A*, Western blot analysis of mitochondrial extracts from *ccs1*Δ::*IMhSOD1* and *ccs1*Δ::*IMhSOD1 pic2*Δ strains, probed with anti-hSOD1 antibody and porin as an internal loading control. *B*, activity of SOD1 in isolated mitochondria from cells grown in synthetic medium with a fermentable carbon source supplemented with 50 μM BCS as measured by xanthine oxidase/tetrazolium salt assay ($n = 3$). There was no detectable SOD1 activity in *ccs1*Δ mitochondria. *C*, activity of SOD1 in isolated mitochondria from cells grown in synthetic medium with a fermentable carbon source supplemented with increasing silver concentrations (20, 40, and 80 μM). *Arb.*, arbitrary; *mito*, mitochondria.

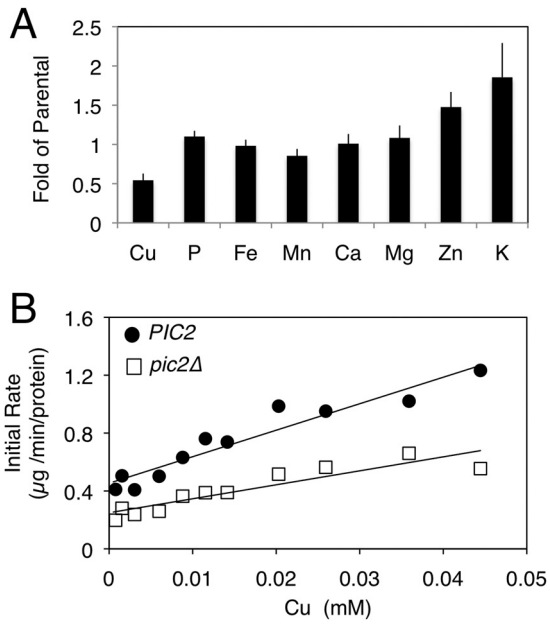

FIGURE 7. **Total mineral element profile and uptake in *pic2*Δ mitochondria.** *A*, overall mineral profile of purified intact mitochondria from *pic2*Δ cells assayed by ICP-OES and compared with that of parental cells. Both strains were grown in medium containing 500 μM copper. The value for each mineral represents the average of ICP-OES analysis of 10 independent mitochondrial preparations, and *bars* represent S.E. *B*, isolated mitochondria from parental or *pic2*Δ cells were assayed for *in vitro* uptake of the CuL. Initial rates of uptake are plotted *versus* variable CuL concentrations. The line is fit by linear regression.

tion suggests a decreased capacity for CuL uptake in the *pic2*Δ strain, consistent with the lower total copper accumulation. This uptake defect was evident across a range of CuL concentrations (Fig. 7*B*). Because Pic2 has been previously identified as a secondary phosphate carrier, mitochondria from *pic2*Δ cells were assayed for phosphate uptake using an established swelling assay (30). Consistent with previous observations, no defect in phosphate uptake was detected in *pic2*Δ mitochondria (data not shown).

Heterologous Expression of Pic2—To account for possible indirect effects of other proteins contributing to the observed defects in mitochondrial copper uptake, we cloned *PIC2* into a nisin-inducible vector for expression in the bacterium *L. lactis*. MCF proteins expressed in *L. lactis* are folded correctly in the cytoplasmic membrane, and transport can be assayed directly in whole cells (31). The presence of Pic2 in *L. lactis* induced with nisin was confirmed by Western blotting using a Pic2-specific antibody (Fig. 8*A*). Expression of *PIC2* enhanced CuL uptake into *L. lactis* compared with cells that carried the empty vector (Fig. 8, *B* and *C*). Addition of a 10-fold excess of phosphate in the form of potassium phosphate buffer did not significantly inhibit copper uptake in the *PIC2*-expressing cells (data not shown). *PIC2* expression in *L. lactis* enhanced the cellular uptake of $CuSO_4$ (Fig. 8*D*) and copper-acetonitrile (data not shown) but did not enhance the uptake of iron presented as $FeSO_4$ (data not shown).

DISCUSSION

Assembly of fully functional CcO depends on a non-proteinaceous pool of labile copper in the mitochondrial matrix (14). Here, we identified Pic2 as the first protein involved in matrix copper import. Yeast cells lacking *PIC2* have copper-related growth defects and a deficit in total mitochondrial copper content. Intact mitochondria from these cells show decreased rates of CuL uptake *in vitro*, and heterologous expression of Pic2 in *L. lactis* supports copper uptake. Taken together, these data support a novel role for Pic2 in mitochondrial copper homeostasis in *S. cerevisiae*.

Total copper in the mitochondria of *S. cerevisiae* is ~50 and 200 μM under fermentative and respiratory growth conditions, respectively (32). Previously, we reported that matrix copper content increases at least 6-fold in response to copper salt supplementation in the medium (11). Therefore, the *in vitro* estimation of 15 μM for half-maximal transport of copper in wild-type mitochondria is likely biologically relevant.

The data presented here suggest that Pic2 mediates CuL import, and under normal physiologic conditions, we believe the CuL to be the major substrate for uptake of the metal ion

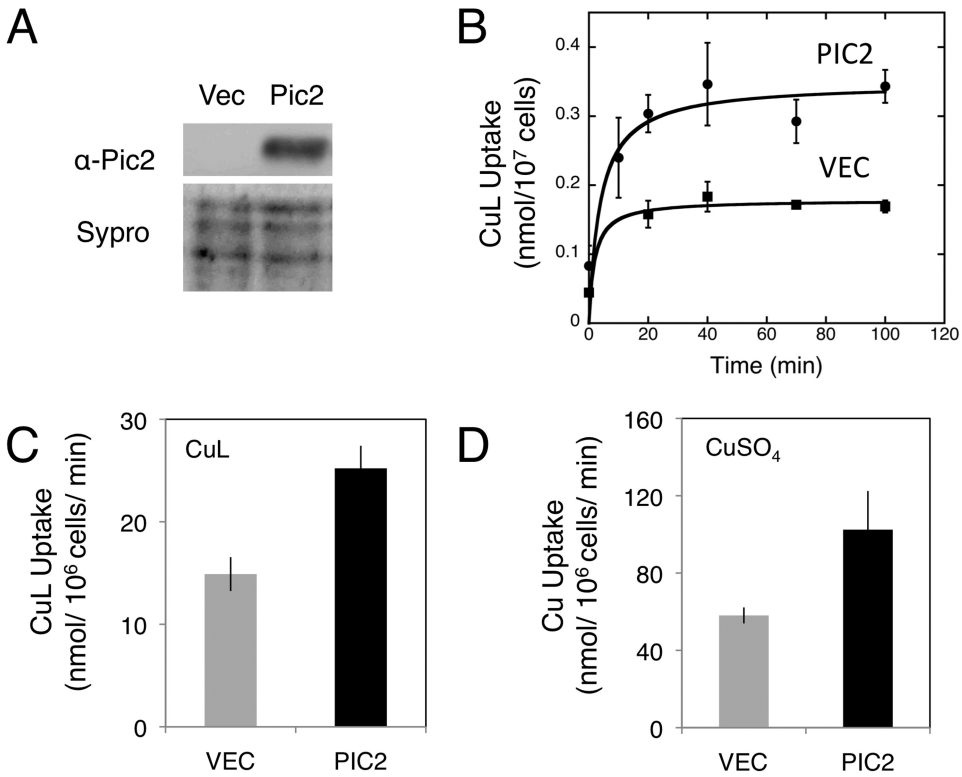

FIGURE 8. **Pic2 expressed in *L. lactis*.** *A,* Western blot analysis of *L. lactis* extracts from cells transformed with either empty vector (*Vec*) or *PIC2* probed with anti-Pic2 antibody after nisin induction. Sypro ruby-stained extracts are shown as loading controls. *B,* uptake of the CuL by intact cells transformed with an empty vector (*Vec*) or *PIC2* incubated at room temperature over time with 20 μM CuL ($n = 4$). *Error bars* represent S.E. Data are fit by a hyperbolic curve. *C*, CuL uptake in cells with either an empty vector or *PIC2* incubated with 10 μM CuL ($n = 3$). *Error bars* represent S.E. *D*, copper uptake in cells with either an empty vector or *PIC2* incubated with 10 μM $CuSO_4$ ($n = 3$). *Error bars* represent S.E.

into the organelle. Apo-ligand appears to be underrepresented in the matrix, suggesting that only the CuL complex is transported across the IM (14). We therefore use the CuL as the source of copper in most of our assays, and this complex is extremely stable under all conditions we have tested, including boiling and organic extraction (14). However, we cannot exclude the possibility that copper dissociates from the ligand for its transport across the IM and rebinds the ligand upon entry into the matrix.

MCF proteins are predicted to contain three α-helices that fold over into a tripartite structure with six membrane-spanning domains (33). Within these helices are conserved P*X*(D/E)*XX*(R/K) motifs, which are proposed to narrow the pore of the carrier and form salt bridges to lock it in a state that is closed to the matrix (15, 33, 34). Substrate binding disrupts these salt bridges and allows for translocation, changing the carrier from an IMS-facing state to a matrix-facing state. Analysis of the sequence of MCF proteins to identify the salt bridges formed within these motifs has been used to predict whether particular family members act as uniporters or strict exchangers (34). The Pic2 salt bridge network in the IMS-facing conformation appears to be stronger than it is in the matrix-facing conformation, consistent with the idea that Pic2 is capable of uniport transport (34). According to the proposed mechanism, it is the greater relative strength of the IMS salt bridge network that drives the protein to revert back to this original conformation after substrate translocation (34). Further experiments with isolated Pic2 will be required to assess the residues required for CuL transport and the exact mechanism of transport.

The phenotypes observed here are most consistent with Pic2 acting as an importer of the CuL, supporting the steady-state level of the CuL in the matrix that is required to activate subsequent transport by an exporter. The expression of matrix-targeted copper competitors does not affect the total levels of copper but does decrease the available CuL, and this induces respiratory defects (14). It is assumed that these competitor copper-binding proteins are able to out-compete the ligand complex for copper binding in the matrix. In *pic2*Δ, this phenotype is exaggerated, presumably because decreased CuL import shifts the equilibrium in favor of the competitor protein(s) whose expression remains constant. To date, we cannot exclude the possibility that Pic2 is capable of bidirectional transport. Analysis of mitochondria from MCF deletion mutants grown under copper-supplemented conditions did not reveal an obvious candidate that significantly overaccumulated copper (data not shown). Therefore, any potential mechanism by which copper import and export may be linked remains unknown.

Defects in transport of ionic copper and iron were previously observed in submitochondrial particles prepared from mutants of the high affinity iron transporters Mrs3 and Mrs4 (16). Similarly, we observed that Pic2 in *L. lactis* can transport $CuSO_4$. Although free copper should not be encountered in the IMS under normal physiologic conditions, this result could explain previous observations of copper accumulation in mitochondria

from cells with compromised copper homeostasis. Deletion of *ACE1*, a copper-regulated transcription factor, in yeast prevents the increase in metallothionein expression normally seen in response to copper supplementation. In this mutant, mitochondrial copper is expanded more dramatically than it is in the parental strain with active Ace1 (11). This increase in copper not only expands the soluble matrix pool but also leads to the accumulation of an insoluble fraction within this mitochondrial compartment, the identity of which has not been investigated. Similarly, mitochondria isolated from a rat model of Wilson disease show accumulation of large quantities of insoluble copper that leads to severe membrane damage (35). It is possible that once copper is no longer bound to the CuL, it can react indiscriminately with various mitochondrial components.

Pic2 has been previously implicated in phosphate transport in yeast, as multicopy *PIC2* could reverse a *mir1*Δ*pic2*Δ growth defect on a non-fermentable carbon source and rescue phosphate transport in *mir1*Δ*pic2*Δ mitochondria as assayed by mitochondrial swelling (30, 36). *PIC2* has also been identified as a high copy suppressor of the mitochondrial K^+/H^+ exchanger mutant (*mdm38*Δ) of yeast (37). The authors concluded that *PIC2* suppressed the defect via rescue of proton-motive force rather that K^+ transport. Interestingly, *MRS3* has also been implicated in transport of ionic copper and also acts as a suppressor of the K^+/H^+ exchanger mutant (37). Whether the role of Pic2 in phosphate and potassium transport has any effect on copper, or vice versa, remains to be investigated.

The cumulative *in vivo* and *in vitro* data argue that Pic2 is a major component of the mitochondrial copper homeostasis machinery. This initial discovery provides a straightforward genetic strategy whereby this null strain can be used to identify additional transporters involved in organellar copper handling. It may also prove to be a useful tool in defining the pathways involved in synthesis of the ligand that binds copper, as a *pic2*Δ strain should be sensitized to modest changes in total CuL content.

Acknowledgments—We thank Shamima Nasrin, Winston Smith, Brigitte Meyers, and Hilliary Street for contributions toward creating necessary reagents and collecting data.

REFERENCES

1. Cobine, P. A., Pierrel, F., and Winge, D. R. (2006) Copper trafficking to the mitochondrion and assembly of copper metalloenzymes. *Biochim. Biophys. Acta.* **1763,** 759–772
2. Huffman, D. L., and O'Halloran, T. V. (2001) Function, structure, and mechanism of intracellular copper trafficking proteins. *Annu. Rev. Biochem.* **70,** 677–701
3. Dancis, A., Yuan, D. S., Haile, D., Askwith, C., Eide, D., Moehle, C., Kaplan, J., and Klausner, R. D. (1994) Molecular characterization of a copper transport protein in *S. cerevisiae*: an unexpected role for copper in iron transport. *Cell* **76,** 393–402
4. Reddi, A. R., and Culotta, V. C. (2013) SOD1 integrates signals from oxygen and glucose to repress respiration. *Cell* **152,** 224–235
5. Tsukihara, T., Aoyama, H., Yamashita, E., Tomizaki, T., Yamaguchi, H., Shinzawa-Itoh, K., Nakashima, R., Yaono, R., and Yoshikawa, S. (1996) The whole structure of the 13-subunit oxidized cytochrome *c* oxidase at 2.8 Å. *Science* **272,** 1136–1144
6. Pufahl, R. A., Singer, C. P., Peariso, K. L., Lin, S. J., Schmidt, P. J., Fahrni, C. J., Culotta, V. C., Penner-Hahn, J. E., and O'Halloran, T. V. (1997) Metal ion chaperone function of the soluble Cu(I) receptor Atx1. *Science* **278,** 853–856
7. Furukawa, Y., Torres, A. S., and O'Halloran, T. V. (2004) Oxygen-induced maturation of SOD1: a key role for disulfide formation by the copper chaperone CCS. *EMBO J.* **23,** 2872–2881
8. Horng, Y. C., Cobine, P. A., Maxfield, A. B., Carr, H. S., and Winge, D. R. (2004) Specific copper transfer from the Cox17 metallochaperone to both Sco1 and Cox11 in the assembly of yeast cytochrome *c* oxidase. *J. Biol. Chem.* **279,** 35334–35340
9. Banci, L., Bertini, I., Ciofi-Baffoni, S., Hadjiloi, T., Martinelli, M., and Palumaa, P. (2008) Mitochondrial copper(I) transfer from Cox17 to Sco1 is coupled to electron transfer. *Proc. Natl. Acad. Sci. U.S.A.* **105,** 6803–6808
10. Horn, D., Al-Ali, H., and Barrientos, A. (2008) Cmc1p is a conserved mitochondrial twin CX9C protein involved in cytochrome *c* oxidase biogenesis. *Mol. Cell. Biol.* **28,** 4354–4364
11. Cobine, P. A., Ojeda, L. D., Rigby, K. M., and Winge, D. R. (2004) Yeast contain a non-proteinaceous pool of copper in the mitochondrial matrix. *J. Biol. Chem.* **279,** 14447–14455
12. Yang, L., McRae, R., Henary, M. M., Patel, R., Lai, B., Vogt, S., and Fahrni, C. J. (2005) Imaging of the intracellular topography of copper with a fluorescent sensor and by synchrotron x-ray fluorescence microscopy. *Proc. Natl. Acad. Sci. U.S.A.* **102,** 11179–11184
13. Dodani, S. C., Leary, S. C., Cobine, P. A., Winge, D. R., and Chang, C. J. (2011) A targetable fluorescent sensor reveals that copper-deficient SCO1 and SCO2 patient cells prioritize mitochondrial copper homeostasis. *J. Am. Chem. Soc.* **133,** 8606–8616
14. Cobine, P. A., Pierrel, F., Bestwick, M. L., and Winge, D. R. (2006) Mitochondrial matrix copper complex used in metallation of cytochrome oxidase and superoxide dismutase. *J. Biol. Chem.* **281,** 36552–36559
15. Kunji, E. R., and Robinson, A. J. (2006) The conserved substrate binding site of mitochondrial carriers. *Biochim. Biophys. Acta* **1757,** 1237–1248
16. Froschauer, E. M., Schweyen, R. J., and Wiesenberger, G. (2009) The yeast mitochondrial carrier proteins Mrs3p/Mrs4p mediate iron transport across the inner mitochondrial membrane. *Biochim. Biophys. Acta* **1788,** 1044–1050
17. Mühlenhoff, U., Stadler, J. A., Richhardt, N., Seubert, A., Eickhorst, T., Schweyen, R. J., Lill, R., and Wiesenberger, G. (2003) A specific role of the yeast mitochondrial carriers MRS3/4p in mitochondrial iron acquisition under iron-limiting conditions. *J. Biol. Chem.* **278,** 40612–40620
18. Shaw, G. C., Cope, J. J., Li, L., Corson, K., Hersey, C., Ackermann, G. E., Gwynn, B., Lambert, A. J., Wingert, R. A., Traver, D., Trede, N. S., Barut, B. A., Zhou, Y., Minet, E., Donovan, A., Brownlie, A., Balzan, R., Weiss, M. J., Peters, L. L., Kaplan, J., Zon, L. I., and Paw, B. H. (2006) Mitoferrin is essential for erythroid iron assimilation. *Nature* **440,** 96–100
19. Wang, Y., Langer, N. B., Shaw, G. C., Yang, G., Li, L., Kaplan, J., Paw, B. H., and Bloomer, J. R. (2011) Abnormal mitoferrin-1 expression in patients with erythropoietic protoporphyria. *Exp. Hematol.* **39,** 784–794
20. Chen, W., Paradkar, P. N., Li, L., Pierce, E. L., Langer, N. B., Takahashi-Makise, N., Hyde, B. B., Shirihai, O. S., Ward, D. M., Kaplan, J., and Paw, B. H. (2009) Abcb10 physically interacts with mitoferrin-1 (Slc25a37) to enhance its stability and function in the erythroid mitochondria. *Proc. Natl. Acad. Sci. U.S.A.* **106,** 16263–16268
21. Paradkar, P. N., Zumbrennen, K. B., Paw, B. H., Ward, D. M., and Kaplan, J. (2009) Regulation of mitochondrial iron import through differential turnover of mitoferrin 1 and mitoferrin 2. *Mol. Cell. Biol.* **29,** 1007–1016
22. Nilsson, R., Schultz, I. J., Pierce, E. L., Soltis, K. A., Naranuntarat, A., Ward, D. M., Baughman, J. M., Paradkar, P. N., Kingsley, P. D., Culotta, V. C., Kaplan, J., Palis, J., Paw, B. H., and Mootha, V. K. (2009) Discovery of genes essential for heme biosynthesis through large-scale gene expression analysis. *Cell Metab.* **10,** 119–130
23. Yang, M., Cobine, P. A., Molik, S., Naranuntarat, A., Lill, R., Winge, D. R., and Culotta, V. C. (2006) The effects of mitochondrial iron homeostasis on cofactor specificity of superoxide dismutase 2. *EMBO J.* **25,** 1775–1783
24. Gordon, D. M., Lyver, E. R., Lesuisse, E., Dancis, A., and Pain, D. (2006) GTP in the mitochondrial matrix plays a crucial role in organellar iron homoeostasis. *Biochem. J.* **400,** 163–168
25. Yoon, H., Zhang, Y., Pain, J., Lyver, E. R., Lesuisse, E., Pain, D., and Dancis, A. (2011) Rim2, pyrimidine nucleotide exchanger, is needed for iron uti-

lization in mitochondria. *Biochem. J.* **440,** 137–146
26. Lin, H., Li, L., Jia, X., Ward, D. M., and Kaplan, J. (2011) Genetic and biochemical analysis of high iron toxicity in yeast. Iron toxicity is due to the accumulation of cytosolic iron and occurs under both aerobic and anaerobic conditions. *J. Biol. Chem.* **286,** 3851–3862
27. Tong, A. H., and Boone, C. (2006) Synthetic genetic array analysis in *Saccharomyces cerevisiae*. *Methods Mol. Biol.* **313,** 171–192
28. Jin, Y. H., Dunlap, P. E., McBride, S. J., Al-Refai, H., Bushel, P. R., and Freedman, J. H. (2008) Global transcriptome and deletome profiles of yeast exposed to transition metals. *PLoS Genet.* **4,** e1000053
29. Zatulovskiy, E. A., Skvortsov, A. N., Rusconi, P., Ilyechova, E. Y., Babich, P. S., Tsymbalenko, N. V., Broggini, M., and Puchkova, L. V. (2012) Serum depletion of holo-ceruloplasmin induced by silver ions *in vivo* reduces uptake of cisplatin. *J. Inorg. Biochem.* **116,** 88–96
30. Hamel, P., Saint-Georges, Y., de Pinto, B., Lachacinski, N., Altamura, N., and Dujardin, G. (2004) Redundancy in the function of mitochondrial phosphate transport in *Saccharomyces cerevisiae* and *Arabidopsis thaliana*. *Mol. Microbiol.* **51,** 307–317
31. Kunji, E. R., Chan, K. W., Slotboom, D. J., Floyd, S., O'Connor, R., and Monné, M. (2005) Eukaryotic membrane protein overproduction in *Lactococcus lactis*. *Curr. Opin. Biotechnol.* **16,** 546–551
32. Garber Morales, J., Holmes-Hampton, G. P., Miao, R., Guo, Y., Münck, E., and Lindahl, P. A. (2010) Biophysical characterization of iron in mitochondria isolated from respiring and fermenting yeast. *Biochemistry* **49,** 5436–5444
33. Pebay-Peyroula, E., Dahout-Gonzalez, C., Kahn, R., Trézéguet, V., Lauquin, G. J., and Brandolin, G. (2003) Structure of mitochondrial ADP/ATP carrier in complex with carboxyatractyloside. *Nature* **426,** 39–44
34. Robinson, A. J., Overy, C., and Kunji, E. R. (2008) The mechanism of transport by mitochondrial carriers based on analysis of symmetry. *Proc. Natl. Acad. Sci. U.S.A.* **105,** 17766–17771
35. Zischka, H., Lichtmannegger, J., Schmitt, S., Jägemann, N., Schulz, S., Wartini, D., Jennen, L., Rust, C., Larochette, N., Galluzzi, L., Chajes, V., Bandow, N., Gilles, V. S., DiSpirito, A. A., Esposito, I., Goettlicher, M., Summer, K. H., and Kroemer, G. (2011) Liver mitochondrial membrane crosslinking and destruction in a rat model of Wilson disease. *J. Clin. Invest.* **121,** 1508–1518
36. Takabatake, R., Siddique, A. B., Kouchi, H., Izui, K., and Hata, S. (2001) Characterization of a *Saccharomyces cerevisiae* gene that encodes a mitochondrial phosphate transporter-like protein. *J. Biochem.* **129,** 827–833
37. Zotova, L., Aleschko, M., Sponder, G., Baumgartner, R., Reipert, S., Prinz, M., Schweyen, R. J., and Nowikovsky, K. (2010) Novel components of an active mitochondrial K^+/H^+ exchange. *J. Biol. Chem.* **285,** 14399–14414